Al-SiC Machinability Studies and Parameter Optimization in Electrical Discharge Machining

[1]Suresh Kumar R, [2]Anijith Raghuvance T, [3]Sathish N, [4]Shre Vijay Raj M and [5]Vigneshkumar M
[1,2,3,4,5] Department of Mechanical Engineering, Sri Eshwar College of Engineering, Coimbatore, Tamil Nadu, India.
[1]rsk777mech@gmail.com

Article Info
S. Venkatesh et al. (eds.), *1st International Conference on Emerging Trends in Mechanical Sciences for Sustainable Technologies*, Advances in Computational Intelligence in Materials Science.
Doi: https://doi.org/10.53759/acims/978-9914-9946-6-7_1

Abstract - Advancement in technology has paved way for new materials and alloys such as Metal Matrix Composites (MMC) that are not only lightweight but possess higher strength-to-weight ratio and hardness. MMCs find applications ranging from nuclear, and aerospace to defence industries. Due to their uniqueness in terms of wear and high-temperature resistance, In industrial applications, these materials are frequently used. The quality of a machined surface is identified by the measure of surface texture achieved in terms of roughness (R_a). Whereas, the production time depends on the rate of production and is directly related to the material removal rate (M_{rr}) of a given process. For achieving best outcome, it is very important to address the above two constraints R_a and M_{rr}. On careful analysis, one can find that these two parameters are contradictory to each other and finding an optimal solution among them is the most crucial task. Conventional machining offers inadequate accuracy and precision while dealing with complicated structures. Also, they are time-consuming and encounter issues while dealing with extremely difficult-to-cut materials. Moreover, localized heating, workpiece stress, and varied cutting forces affect the overall performance of the operation. To address such issues, electrical discharge machining (EDM) offers a controlled electric spark that nearly generates strong cutting force, minimal stress on the workpiece surface during high flexibility and material removal, which has recently gained attention as a technology that is efficient for cutting materials that are challenging to work with. But still, from a techno-economical perspective, achieving higher efficiency is crucial due to the complex-dynamic relationship of the parameters involved in the EDM process. This article deals with the machinability performance and its optimization of Al-SiC alloy while performing machining operations in EDM by considering Pulse on, Wire Feed, Pulse off and Servo voltage as the controlling parameters. The responses considered were R_a, $M_{rr.}$

Keywords - Al-SiC, Electrical Discharge Machining, Roughness, Pulse on (A), Wire Feed (C), Pulse off (B) and Servo Voltage (D).

I. INTRODUCTION

The field of science and technology has been continuously pushing the boundaries for the development of new materials and compositions that possess high hardness, strength with reduced weight. Metal matrix composites (MMC) have gained increasing popularity in industries including electronics, aerospace, automotive, defence, and nuclear compared to conventionally available materials. These are extensively considered due to their high performance in terms of desirable properties required, but traditional machining techniques often fall short in terms of accuracy, precision, and efficiency when it comes to machining MMCs, which can have complex shapes and be time-consuming or even impossible to machine. In recent times, EDM has emerged as an effective means for machining hard materials, including MMCs, due to its controlled electric spark in localized means generating minimal cutting force and stress while machining. Therefore, EDM has become a sustainable and viable alternative for machining MMCs. However, achieving high production efficiency in EDM requires careful consideration of input parameters that controls the EDM process. To name few of the input parameters includes dielectric flushing pressure, electrode used, dielectric fluids, pulse duration etc. Moreover, optimizing the EDM process for different materials requires a systematic approach that combines experimental, modeling, and optimization methodologies to address the multiple conflicting objectives (multi-objective) involved in the process. Several statistical and computational approaches, such as Artificial Neural Networks (ANN), Grey Relational Analysis (GRA), Taguchi Design (TD), Desirability Function Approach (DFA), Principal Component Analysis (PCA), Response Surface Methodology (RSM), Genetic Algorithm (GA), and Particle Swarm Optimization (PSO) etc. have been applied for predictive modeling and process optimization in EDM. While extensive research has been conducted on different workpiece materials using these statistical tolls still there is a lack of studies on the machining characteristics for Al-SiC based MMCs using EDM. Furthermore, most of the literature has focused on major machining performance indicators like M_{rr}, electrode wear rate, and R_a, while neglecting other important aspects, such as

cracking of surfaces and thickness of recast layer. Moreover, there is a gap in the literature in terms of economic analysis to enable cost-efficient EDM machining, which presents an opportunity for further research from a techno-economic perspective. Additionally, sustainability assessment in the EDM process, which aligns with the current trend towards green and cleaner manufacturing practices for a safer environment, remains largely unexplored. In light of these research gaps and the potential contributions to the field, this study analyzes the EDM efficiency while working on Al-SiC in terms of M_{rr}, and R_a, with controlling parameters as discharge current, A, B, C and D. The study utilize Box-Behnken design (BBD), Analysis of Variance (ANOVA), RSM, and computational approaches to develop an effective and optimized machining model using EDM. The study will also consider the techno-economic aspect by analyzing the economic feasibility of the EDM process for cost-effective manufacturing.

II. LITERATURE SURVEY

Advancement in Science & Technology has surfaced the way for new materials and alloys such as Metal Matrix Composites (MMC) that are not only lightweight but possess higher strength-to-weight ratio and hardness. MMCs find its application ranging from nuclear, and aerospace to defence industries. Due to their uniqueness in terms of wear and high-temperature resistance, MMCs are widely used in industrial applications.

The measure of surface texture represents the quality of a machined surface is measured in terms of R_a. Whereas, the production time depends on the rate of production and is directly related to the M_{rr} of a given process. For achieving best outcome, it is very important to address the above two constraints Ra and M_{rr}. On careful analysis, one can find that these two parameters are contradictory to each other and finding an optimal solution among them is the most crucial task. Conventional machining offers inadequate accuracy and precision while dealing with complicated structures. Also, they are time-consuming and encounter issues while dealing with extremely difficult-to-cut materials. Moreover, localized heating, workpiece stress, and varied cutting forces affect the overall performance of the operation. To address such issues, electrical discharge machining (EDM) offering a controlled electric spark producing required cutting force, minimal stress on the machining surface has recently gained attention as an effective technology for machining. But still, from a techno-economical perspective, achieving higher efficiency is crucial due to the complex-dynamic relationship of the parameters involved in the EDM process. Several research has been conducted in EDM for understanding the behaviour of machinability and the impact of the process parameters considered for the investigations. Dielectric flushing pressure is one of several parameters that determine how the cutting process performs in EDM [1], which also includes electrode materials [2–4], factors that impact electric sparks [current (D_c), discharge voltage (D_v), frequency (f), and pulse length (P_l)] [5–7] and dielectric fluids [8–9]. In addition, identifying appropriate and ideal parameters for EDM plays a crucial role that offers improved machining outcomes in terms of efficiency in-built with higher quality and reduced machining cost. EDM is indeed a suitable process for milling advanced composites made of metal matrix materials. It utilizes electrical discharges to remove material and shape the workpiece. It offers several advantages and capabilities that make it well-suited for working with advanced composites. Different statistical and computational techniques, which include RSM [10–11], ANN has been used in predicted modelling and Taguchi method [12], GRA [13–14], Affordability requirement approach of RSM [15–16], PCA [17–18], TOPSIS [19–20], GA [21], and PSO [22–23] have been used for process and parametric optimization of EDM. The machinability has been the subject of many tests using a variety of experimental concepts, computational methods, and optimization techniques [24–25], to predict different technical responses and control process parameters while cutting various workpiece materials (Al-Mg2Si, MDN 300, Al-SiC MMC, AISI 316 L, Ti13Zr13Nb, nickel alloy, Al7075, Al6061, Al6063 alloy, Si3N4-TiN MMC, WC,Ti6Al4V, AISI D2, D3, D6).

Since multiple attempts have been made by researchers around the world to identify the machining characteristics and associated procedure variables to manage the requirements for EDM, extra study is still needed to analyze the results of different EDM parameters and increase material effectiveness. The literature review shows that no significant experiments were done on the use of the EDM methodology to process hard-to-machine materials, such as Al-SiC based on MMC. Further, it was noticed that a majority of the literature focuses primarily on characteristics such as $M_{rr,}$ and R_a of the machined component when evaluating machining performance; problems such as surface cracks and layer width in recasting were not stressed as much. The study reveals a number of investigations that have been published that use either a single approach (computational or statistical) but not addressed multi-objective issues, which are inevitable in enhancing the productivity and machining performance. Therefore, it is essential to set up a suitable technical framework for Al-SiC to arrive at efficient and ideal machining while using EDM. Comparatively, almost no researcher has developed an economic analysis approach that enables cost-effective manufacturing utilizing EDM. This makes the current investigation suitable for further investigation. The objective is to analyse the efficiency of EDM while working on Al-SiC in terms of M_{rr}, and R_a by appropriate controlling factors (D_c, A, B, F_p). In the study BBD is used to perform experimental runs followed by ANOVA and application of GRA to arrive at optimized solution. The study will be helpful as technological guidance for the industrial usage in the automotive, aerospace, military, and electrical sectors working on the workpiece considered for study.

III. BOX-BEHNKEN DESIGN (BBD)

BBD was developed by E. P. Box and Donald Behnken as a response surface methodology experimental design. It aims to achieve three equally spaced values for each variable, with a minimum of three levels required. The design is quadratic in nature, incorporating terms consisting of squares, products of two factors, intercepts, and linear terms. The ratio between the number of experimental points and coefficients should ideally fall between 1.5 to 2.6 for optimal performance. BBD is widely considered as the most powerful due to its superior coverage of non-linear design space and corners. It is an independent quadratic design with an embedded factorial known as a response surface design. These designs require 3levels of each factor resulting in a higher-order response with fewer experimental runs compared to other traditional techniques.

To ensure accuracy and prevent errors, the number of runs conducted should not be overly large under steady-state conditions. The number of factors or parameters under study determines the size of blocks to be added. Every design includes orthogonal blocks, and BBD specifically requiring only three levels. Two-level factorial designs with the necessary statistical properties were employed for sequential runs to be performed. The quadratic model is appropriate with only three levels, and blocking options are often available with these designs, allowing for the generation of runs to be multiplied.

Box Behnken Steps

- The design entails specified points for positioning factors.
- Each factor is assigned three levels.
- A quadratic model is utilized for estimating the design.
- Strong coefficient estimates are located precisely at the centre point of the design and weaker coefficients positioned at the corners of the cube.
- Caution must be exercised as missing data and runs can potentially introduce inaccuracies in the results, rendering the Box-Behnken method not recommended.
- The Central Composite Design (CCD) is often preferred due to its inclusion of more initial runs and better suitability for problem-solving.

IV. GREY RELATIONAL ANALYSIS (GRA)

Normalization

The approach utilized in the data preparation stage is determined by the objective function selected. Equation (1) is applied for normalization when the aim is to maximize a parameter, while Equation (2) is used when the goal is to minimize a parameter. Normalization, a statistical method that standardizes data to a consistent scale, is employed to reduce variance and simplify analysis. The selection of the objective function in the data preparation stage guides the normalization approach, with Equation (1) for maximizing and Equation (2) for minimizing parameters, in order to achieve consistency in data analysis.

$$Yi(k) = \tag{1}$$

$$Yi(k) = (maxyi(k) - yi(k))/(maxyi(k) - minyi(k)\,) \tag{2}$$

Here, i= 1,..... j; k = 1,..... k. j is the experimental data. k represents the responses. Yi(k) denotes value after data pre-processing, while yi(k) is the original data (sequences). Max yi(k) and min yi(k) are the largest and minimal value of yi(k).

Deviation Sequence

Smaller-the-better option is opted for R_a and the larger-the-better for M_{rr}. The deviation calculated by determining the difference between each response and the highest normalized value obtained, proportionate to that value.

Grey Relational Coefficients (GRCs)

GRC, ξi(l) are calculated using equation. Absolute value is reflected based on the minimum and maximum values recorded. Typically the value ranges between 0 and 1, and in this study the differentiating coefficient is set at 0.5.

$$\xi i(l) = (\Delta min + \Psi \Delta max)/(\Delta oi(l) + \Psi \Delta max) \tag{3}$$

Grey Relational Grade (GRD)

GRD (c) represents the correlation between the reference value and comparison sequences. In this stage, a multi-objective function is transformed into a single-objective function and GRD is calculated using the equation 4.

Optimal Parameters

The rank of each group of values is determined in this stage. By using the attained rank, the optimal level can be computed efficiently, consolidating all responses to identify the best alternative.

Optimized set of Parameters using GRA

GRA is utilized to calculate the correlation between the observations, M_{rr} and R_a, and obtain a ranked grade that represents the best possible outcome of the parameter combination. The highest ranked grade is selected to obtain the optimal results.

V. EXPERIMENTAL WORK

Material

In the current study, Al-SiC has been chosen as the material of choice. Al-SiC finds widespread applications in various industries such as aerospace, automotive, marine, owing to its favorable strength-to-weight ratio, as well as its use in screws and bolts. The chemical constituents of the material are enlisted in **Table 1**.

Table 1. Chemical Composition

Al	Cu	Si	Mg	Fe	Ti	Cr	Mn	Zn	Others
96.85	0.3	0.7	0.9	0.6	0.10	0.25	0.05	0.20	0.05

Machine and Tools

The machining operation was performed on a 4-Axis wire EDM, and an electrode of 0.4 mm diameter was employed while machining. The experimental runs were performed based on Box Behnken design with assigned parameters as enlisted in **Table 2** with their levels assigned.

Table 2. Machining Parameters

Name	Notations	Levels		
		1	2	3
Pulse ON (µm)	A	3	8	12
Pulse OFF(µm)	B	10	15	20
Wire Feed (m/min)	C	2	3	4
Servo Voltage (V)	D	35	40	45

Experimental Runs

Table 3 enlists the experimental runs performed with their responses as per the sequence of runs specified by BBD.

Table 3. Experimental Runs with Responses

Run	A (µs)	B (µs)	C (m/min)	D (V)	R_a (µm)	M_{rr} (mm^3/min)
1	3	15	4	40	0.412	0.000384
2	8	15	3	40	0.901	0.002475
3	8	20	3	35	1.253	0.000484
4	12	15	2	40	0.269	0.00383
5	8	20	3	45	0.637	0.002188
6	3	10	3	40	0.331	0.001158
7	8	15	3	40	0.198	0.001916
8	8	10	4	40	1.426	0.001204
9	8	10	3	45	1.287	0.001259
10	12	15	3	35	0.783	0.001531
11	12	15	3	45	0.582	0.002922
12	8	10	2	40	0.173	0.001638
13	8	20	4	40	0.641	0.00053
14	12	20	3	40	0.905	0.003371
15	8	15	4	35	1.232	0.000392
16	8	15	2	35	0.104	0.003478
17	8	15	4	45	0.266	0.00165

18	8	15	3	40	1.259	0.001455
19	8	15	3	40	1.048	0.001543
20	12	15	4	40	1.165	0.001719
21	3	15	3	35	0.389	0.000557
22	8	20	2	40	0.119	0.001914
23	3	15	3	45	0.683	0.000294
24	8	15	2	45	1.388	0.000369
25	12	10	3	40	1.491	0.00049
26	8	15	3	40	1.342	0.002377
27	3	15	2	40	0.284	0.000402
28	3	20	3	40	0.873	0.001896
29	8	10	3	35	0.67	0.002579

Surface Tester

R_a is measured using a Mitutoyo surface tester, and the average R_a value is recorded for analysis.

VI. RESULT AND DISCUSSION

ANOVA for R_a

The ANOVA for R_a and the F-value (2.51) shows the significance of the model developed. This value represents that the model has only a 4.86% chance of attaining this value due to noise factor considered (**Table 4**).

Table 4. ANOVA for R_a

Source	Sum of Squares	df	Mean Square	F-value	p-value	
Model	4.1	14	0.2927	2.51	0.0486	significant
A	0.4118	1	0.4118	3.52	0.0816	
B	0.0396	1	0.0396	0.3383	0.57	
C	0.5706	1	0.5706	4.88	0.0444	
D	0.0222	1	0.0222	0.1896	0.6699	
AB	0.3327	1	0.3327	2.84	0.1138	
AC	0.1425	1	0.1425	1.22	0.2883	
AD	0.0596	1	0.0596	0.5092	0.4872	
BC	0.1336	1	0.1336	1.14	0.3033	
BD	0.3801	1	0.3801	3.25	0.093	
CD	1.27	1	1.27	10.82	0.0054	
A^2	0.1584	1	0.1584	1.35	0.2639	
B^2	0.0049	1	0.0049	0.0419	0.8407	
C^2	0.45	1	0.45	3.85	0.07	
D^2	0.0099	1	0.0099	0.0844	0.7757	
Residual	1.64	14	0.117			
Lack of Fit	0.8108	10	0.0811			
Pure Error	0.8267	4	0.2067			
Cor Total	5.74	28				

The significance of the parameters can be ascertained by the p-value at 90% confidence interval. Here in this case P-value (less than 0.0500) shows that the model generated is significant. In this case C, CD are significant model terms. The governing equation of R_a is given in Eqn 5 below.

$$Ra = -29.92995 + 0.440952 * A + 0.654018 * B + 6.53507 * C + 0.696450 * D - 0.012765 * A * B + 0.041773 * A * C - 0.005401 * A * D - 0.036550 * B * C - 0.012330 * B * D - 0.112500 * C * D - 0.007840 * A * A + 0.001100 * A * A - 0.263383 * C * C - 0.001560 * D * D \ldots\ldots\ldots \quad (5)$$

Parameter Interaction Effects on R_a

The following figures illustrate the interaction effects of the parameters on R_a, providing a clear understanding of how the parameters impact the responses and aiding in the selection of optimal machining parameters based on the assigned objectives. **Fig 1** depicts the interaction effect of A and B on R_a. The graph shows that the minimum R_a can be achieved within the range of 3 to 4 µs, depending on the level of B. As the level of B increases from 13 µs, there is a gradual and significant increase in R_a. However, the lowest R_a is achieved when A is maintained at lower levels and B between 10 to 13 µs. **Fig 2** depicts the interaction effect of A and D on R_a. The graph shows that the minimum R_a can be achieved within the range of 3 to 4 µs for A, and 35 to 37 V for D. Other combinations of levels resulted in higher R_a. This interprets that the influence of A and D are the prominent factors in governing the R_a.

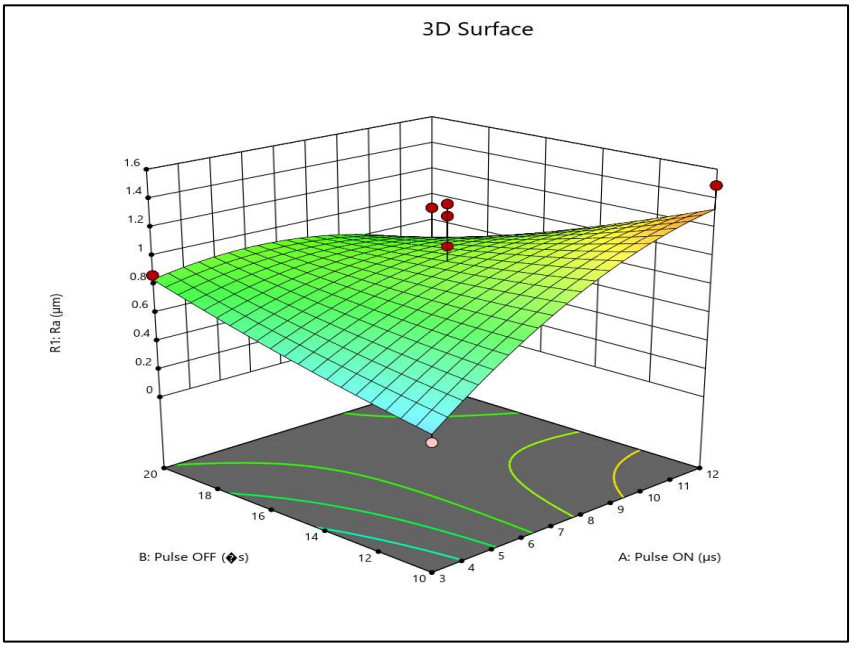

Fig 1. Interaction Plot of A, B on R_a.

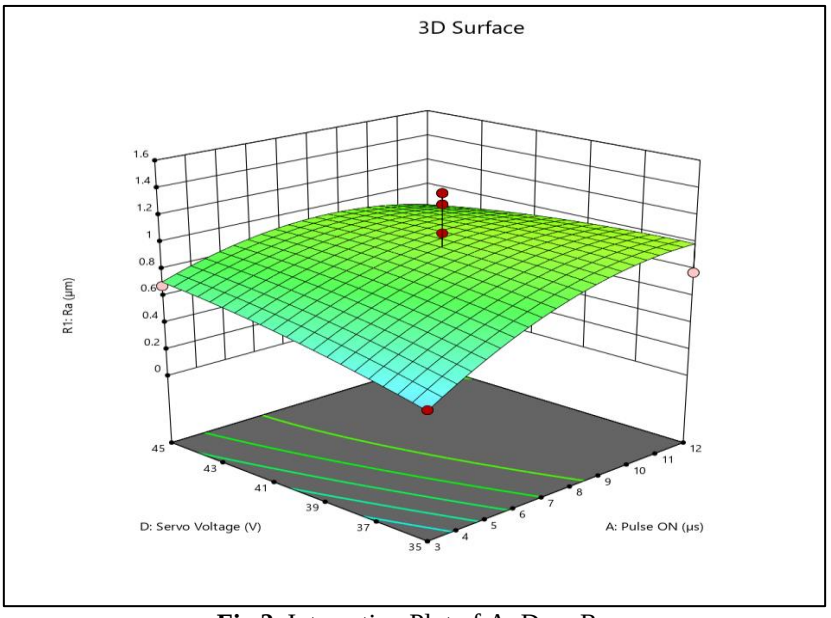

Fig 2. Interaction Plot of A, D on R_a.

Fig 3 depicts the interaction effect of A and C on Ra. The graph shows almost all levels of A contributes towards minimum Ra. However, it is being influenced by the factor C. The lower level of C contributes well in achieving the desired response. When the level of C is increased beyond 2.3 m/min one could witness a gradual increase in Ra.

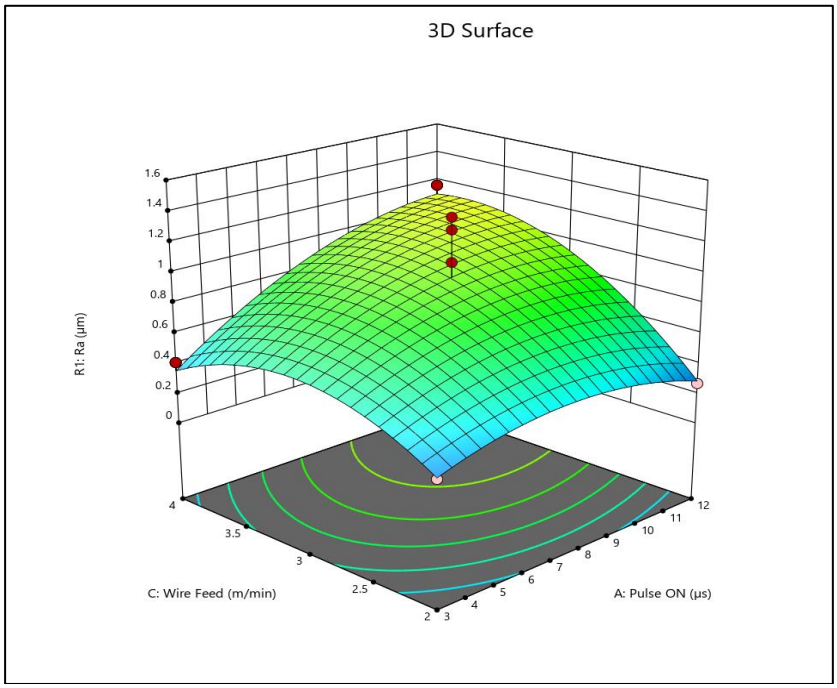

Fig 3. Interaction Plot of A, Con R_a.

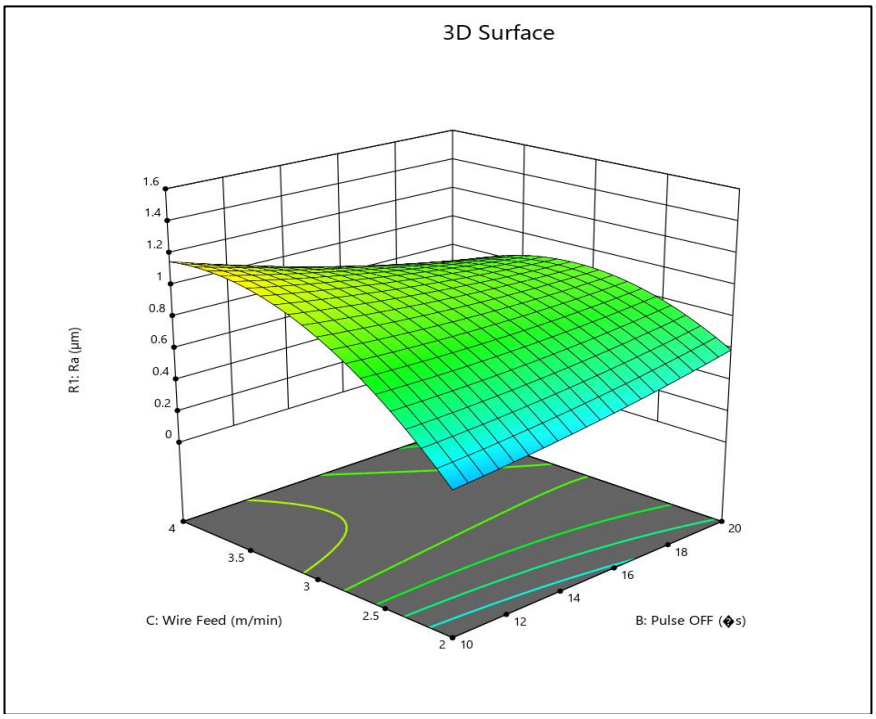

Fig 4. Interaction Plot of B, C on R_a.

Fig 4 depicts the interaction effect of B and C on R_a. Minimum R_a is achieved when B is maintained between 10 to 14 µs and C maintained at lower level of 2 m/min. Any other combination of levels resulted in higher R_a that proves the contradictory effect of these two parameters in governing the output response of R_a.

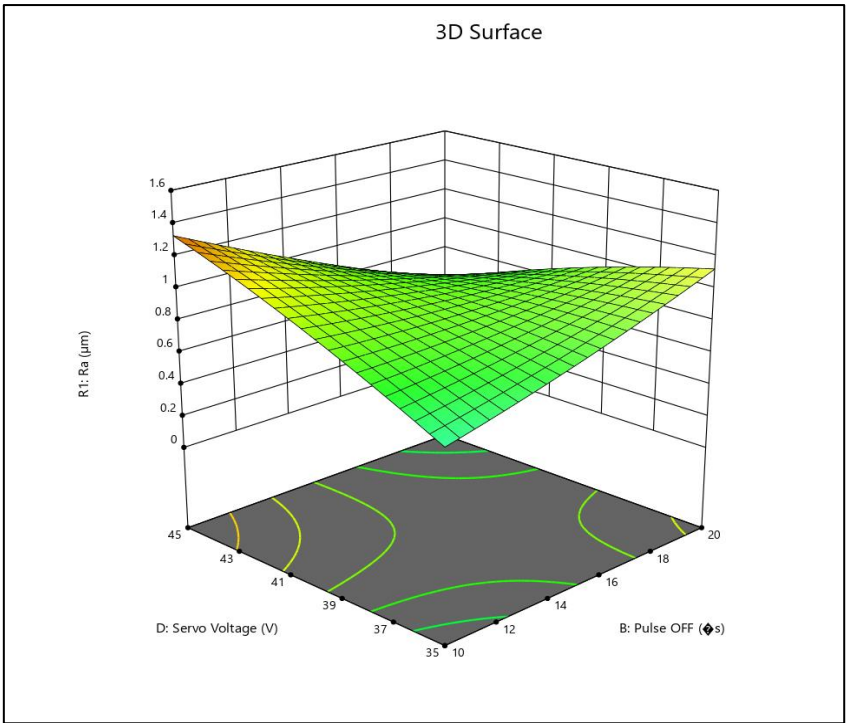

Fig 5. Interaction Plot of B, D on R_a.

Fig 5 depicts the interaction effect of B and D on R_a. From the graph, it can be predicted that these two parameters are the prominent factors governing the response. The minimum Ra that could be achieved in best possible combination of these two factors is around 0.2 microns. Hence in identifying the optimal solutions the interaction effect of these two factors is inevitable. **Fig 6** depicts the interaction effect of C and D on R_a. The graph shows that when C is maintained between 2 to 2.3 m/min and D between 35 to 37 V resulted in minimum R_a.

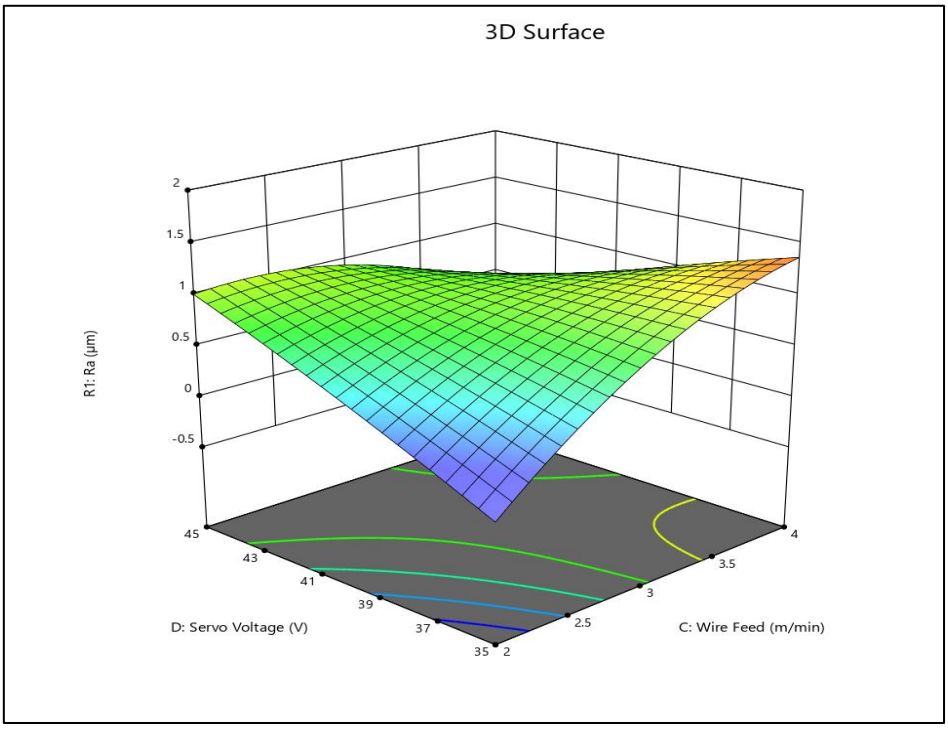

Fig 6. Interaction Plot of C, D on R_a.

Predicted Optimum Parameter for R_a

The below **Table 5** displays the predicted optimized value for R_a

Table 5. Optimized Value - R_a

A	B	C	D	R_a
7.207	19.169	3.893	44.807	0.07

Prediction of M_{rr}

Table 6 shows the ANOVA for M_{rr} and the F-value (2.49) shows the significance of the created and developed model. This value represents that the layout or model has only a 4.94% chance of attaining this value due to noise factor considered.

Table 6. ANOVA for M_{rr}

Source	Sum of Squares	df	Mean Square	F-value	p-value	
Model	0	14	1.49E-06	2.49	0.0494	significant
A	7.01E-06	1	7.01E-06	11.75	0.0041	
B	2.25E-07	1	2.25E-07	0.3763	0.5494	
C	2.30E-06	1	2.30E-06	3.86	0.0698	
D	3.72E-08	1	3.72E-08	0.0623	0.8065	
AB	8.19E-07	1	8.19E-07	1.37	0.2609	
AC	1.06E-06	1	1.06E-06	1.78	0.2034	
AD	5.70E-07	1	5.70E-07	0.9555	0.3449	
BC	2.26E-07	1	2.26E-07	0.3783	0.5484	
BD	2.29E-06	1	2.29E-06	3.83	0.0705	
CD	4.77E-06	1	4.77E-06	7.99	0.0134	
A^2	4.37E-08	1	4.37E-08	0.0733	0.7905	
B^2	1.42E-07	1	1.42E-07	0.2372	0.6338	
C^2	5.75E-07	1	5.75E-07	0.9645	0.3427	
D^2	4.86E-07	1	4.86E-07	0.8145	0.382	
Residual	8.35E-06	14	5.97E-07			
Lack of Fit	7.48E-06	10	7.48E-07			
Pure Error	8.70E-07	4	2.17E-07			
Cor Total	0	28				

The significance of the parameters can be ascertained by the p-value at 90% confidence interval. Here in this case P-value (less than 0.0500) shows that the model generated is significant. In this case A and CD are significant model terms. The governing equation of R_a is given in Eqn 6 below.

$$\text{Mrr} = +0.027106 - 0.000395 * A - 0.001012 * B - 0.005821 * C - 0.000369 * D + 0.000020 * A * B - 0.000114 * A * C + 0.000017 * A * D - 0.000048 * B * C + 0.000030 * B * D + 0.000218 * C * D - 4.11912E-06 * A * A - 5.90733E-06 * B * B - 0.000298 * C * C - 0.000011 * D * D \ldots\ldots\ldots \quad (6)$$

Parameter Interaction Effect on M_{rr}

The following figures represents the interaction effects of the parameters on M_{rr}. This set of representation gives a clear understanding the parametric effect on the result and outcome, which in turn helps to optimize the machining parameter selection based on the objectives assigned. **Fig 7** depicts the interaction effect of A and B on R_a. The graph shows that the maximum M_{rr} is achieved when A is maintained at level between 8 to 12 µs, and at higher level of 20 µs. The graphical representation shows contribution towards higher Mrr except when the level of B is assigned between 16 to 20 µs and A maintained at lower level of 2 µs. This relationship shows the contradictory performance of the two factors towards Mrr.

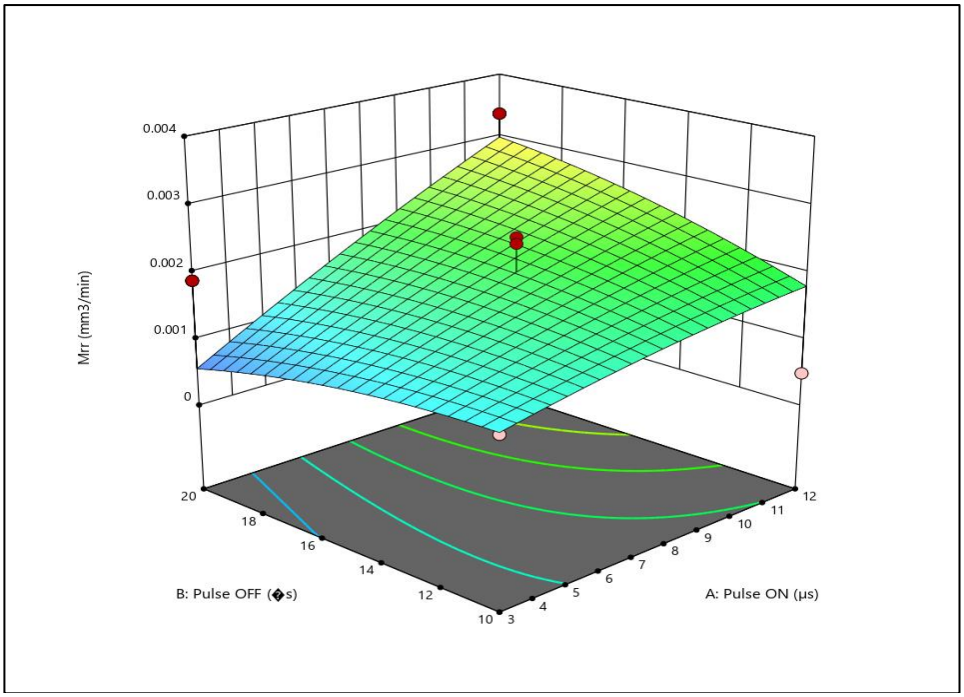

Fig 7. Interaction Plot of A, B on $M_{rr.}$

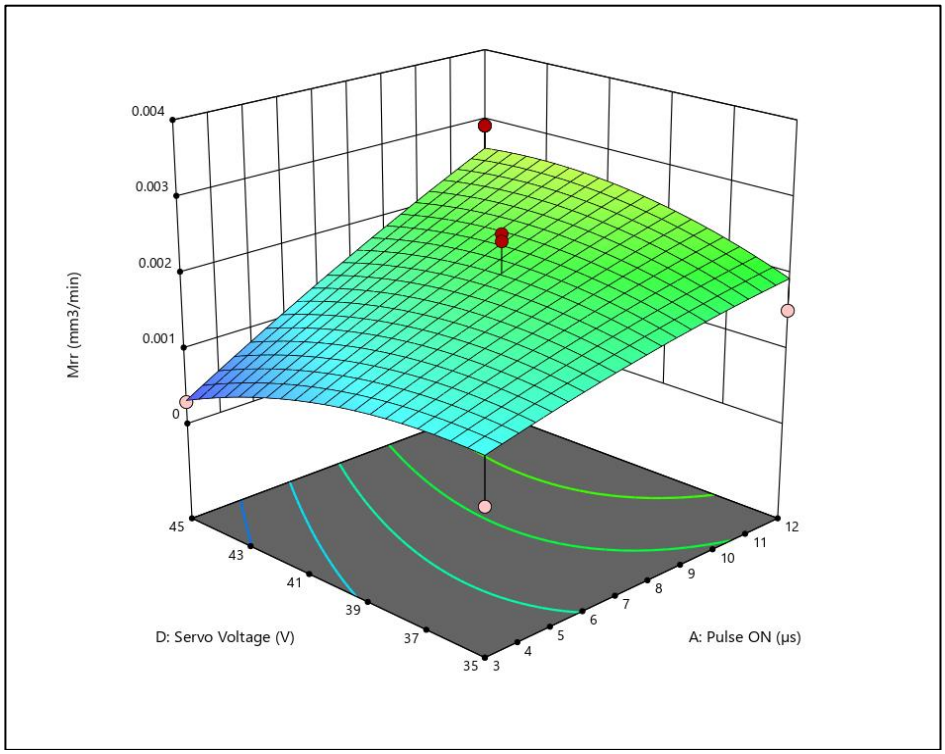

Fig 8. Interaction Plot of A, D on $M_{rr.}$

Fig 8 depicts the interaction effect of A and D on M_{rr}. The graph shows that the higher M_{rr} can be achieved within the range of 10 to12 µs for A, and 40 to 45 V for D. **Fig 9** depicts the interaction effect of A and C on M_{rr}. The graph shows that higher level of A contributes towards maximum Mrr. However, it is being influenced by the factor C. The lower level of C contributes well in achieving the desired response. When the level of C is increased beyond 2.5 m/min one could witness a gradual decrease in M_{rr}.

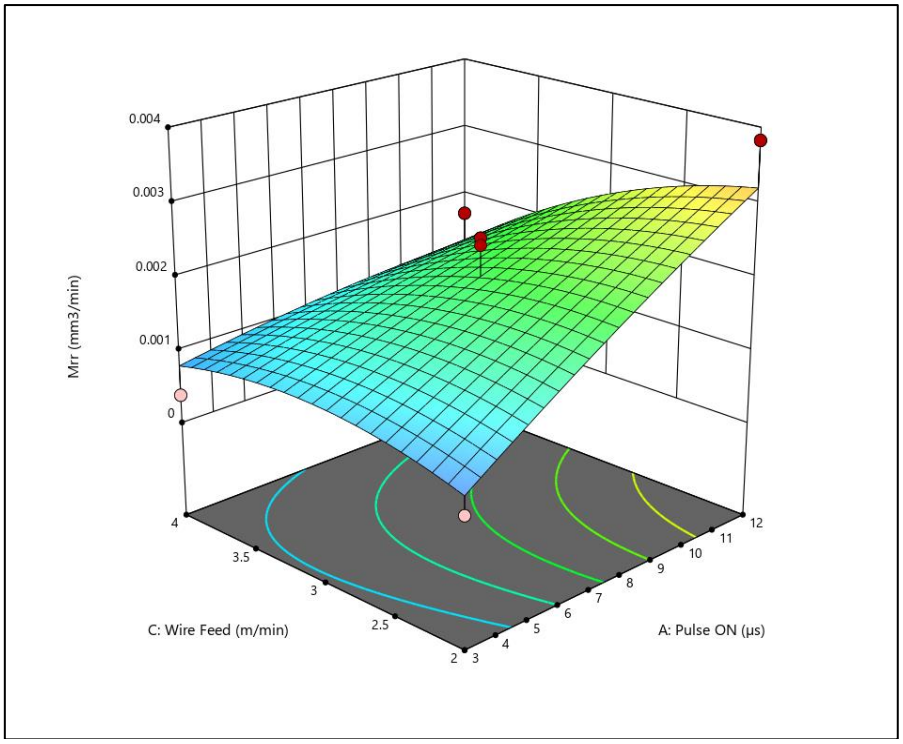

Fig 9. Interaction Plot of A, C on M_{rr}.

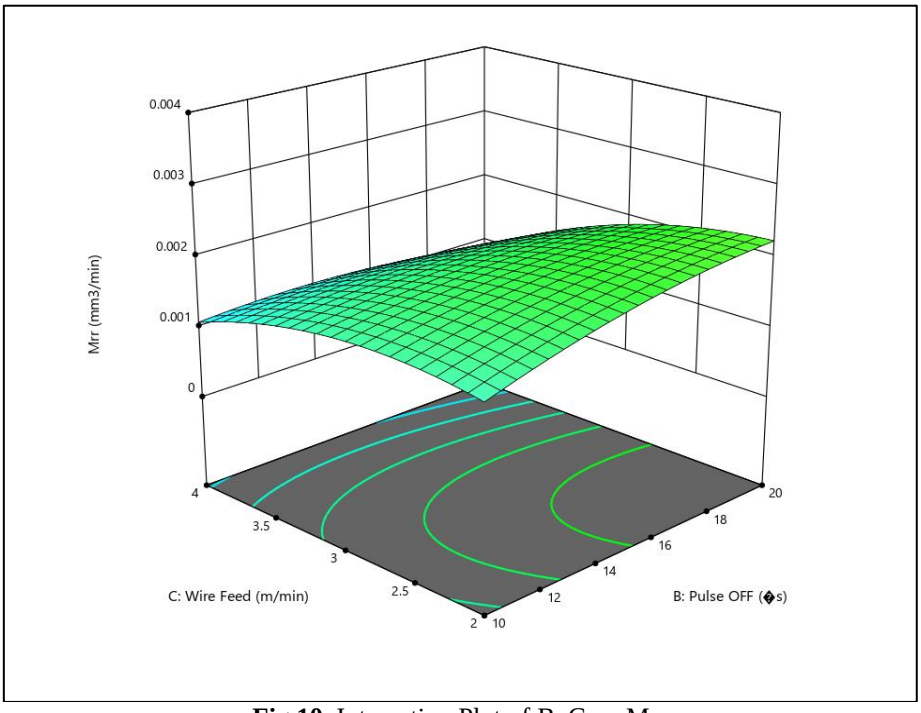

Fig 10. Interaction Plot of B, C on M_{rr}.

Fig 10 depicts the interaction effect of B and C on M_{rr}. The graph shows that almost in all assigned levels of B and C contributes toward achieving maximum M_{rr}. This proves that the factors B and C plays a very vital role in determining the response actively. **Fig 11** depicts the interaction effect of B and D on M_{rr}. From the graph, it can be predicted that maximum Mrr is achieved when B is assigned between 10 to 17 µs and D assigned between 35 to 43 V. **Fig 12** depicts the interaction effect of C and D on M_{rr}. Maximum M_{rr} is achieved when C is maintained between 2 to 3.3 m/min and D between 35 to 45 V.

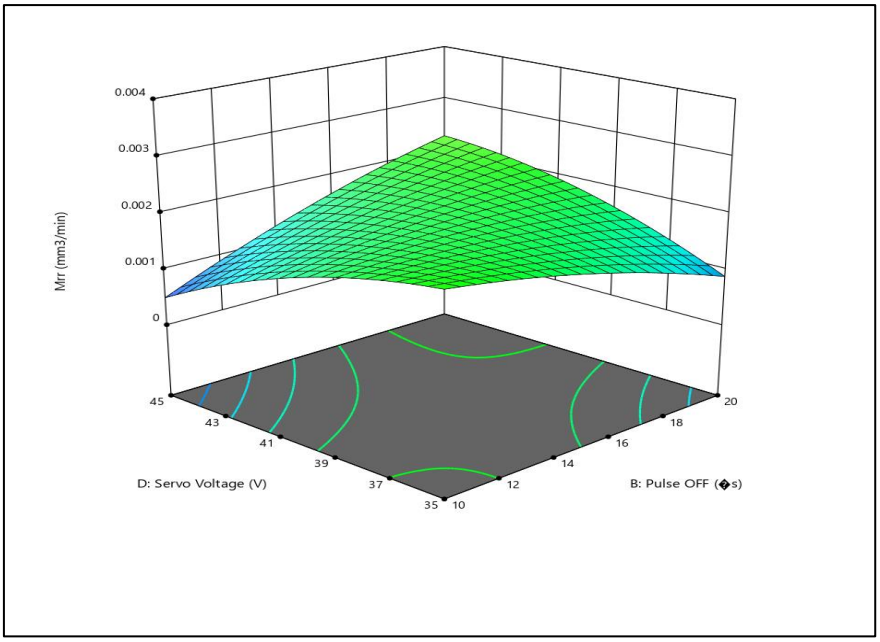

Fig 11. Interaction Plot of B, D on $M_{rr.}$

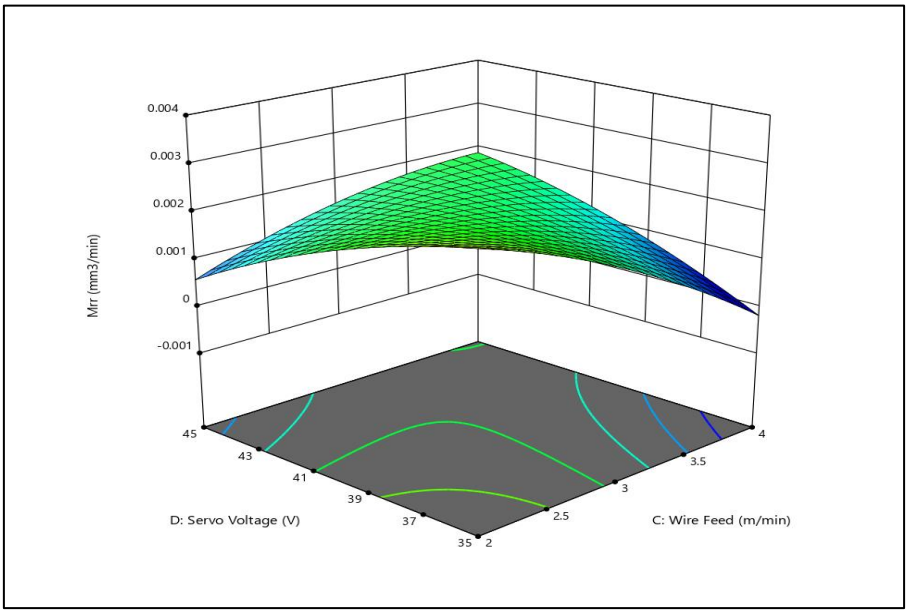

Fig 12. Interaction Plot of C, D on $M_{rr.}$

Predicted Optimum Parameter for M_{rr}

The below **Table 7** shows the predicted optimized value for M_{rr} based on BBD design.

Table 7. Optimized Value - M_{rr}

A	**B**	**C**	**Servo Voltage**	**M_{rr}**
11.961	19.932	2.011	38.866	0.004

VII. SEM Analysis

The following section provides an explanation of the SEM images taken for the experimental runs conducted to further interpret the surface texture achieved by EDM. SEM analysis was performed as shown in the subsequent sections. **Fig 13** displays the SEM images for runs 10, 12, 16, 17 and 18 at a magnification level of 500X. In all the images, there is evidence of adhered material fragments that develop during plastic deformation while machining. Smeared materials, micro holes, and grooves are also visible in the images, which are formed during the material removal process and are consistently present throughout. The presence of burrs and adhered chip particles is possibly due to thermal distortion or inefficient removal of temperature that arises due to EDM process.

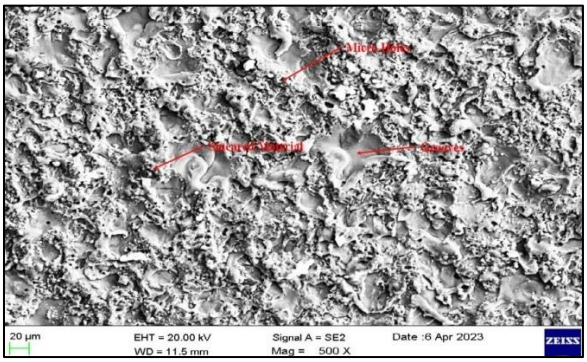

a) Run 10

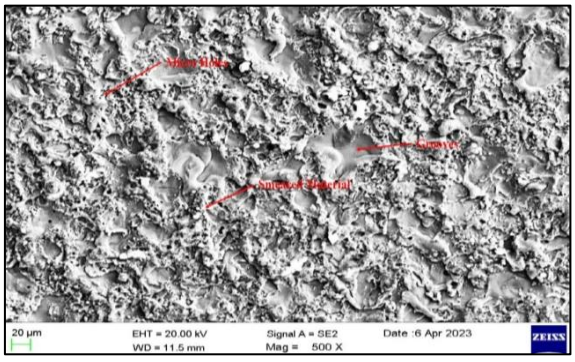

b) Run 12

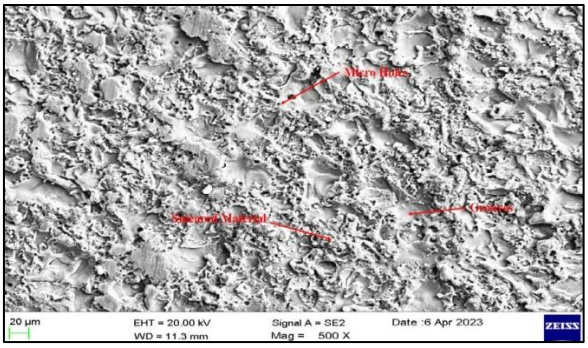

c) Run 16

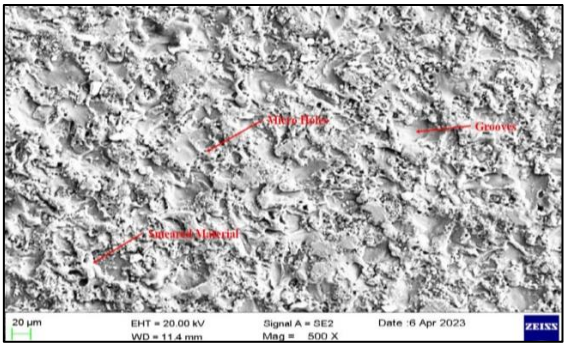

d) Run 17

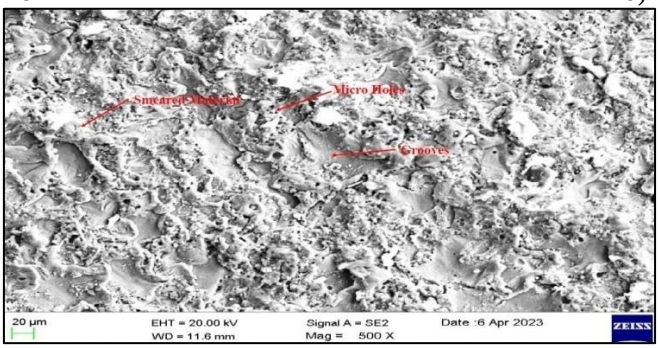

e) Run 18

Fig 13. SEM Images.

VIII. GRA Optimization

Table 8 presents the computation of the GRA for the responses recorded from the experimental runs conducted. The data was first normalized and then deviation sequencing was performed. In the third stage, the grey relation coefficient was calculated, followed by the determination of ranks based on the computed GRG values. The analysis reveals that run 1 has the highest rank and is selected as the optimized values for this machining process, considering all responses in the multi-objective optimization.

Table 8. GRA Optimization

R_a	M_{rr}	Normalized Values		Deviation Sequence		Grey Relation Coefficients		GRG	Rank
		R_a	M_{rr}	R_a	M_{rr}	R_a	M_{rr}		
0.412	0.000384	0.778	0.973	0.222	0.026	0.692	0.951	0.822	2
0.901	0.002475	0.425	0.383	0.575	0.616	0.465	0.448	0.457	27
1.253	0.000484	0.172	0.945	0.828	0.054	0.376	0.903	0.640	14
0.269	0.00383	0.881	0.000	0.119	0.999	0.808	0.334	0.571	16
0.637	0.002188	0.616	0.464	0.384	0.535	0.565	0.483	0.524	18

0.331	0.001158	0.836	0.755	0.164	0.244	0.753	0.672	0.713	8
0.198	0.001916	0.932	0.541	0.068	0.458	0.881	0.522	0.701	9
1.426	0.001204	0.047	0.742	0.953	0.257	0.344	0.660	0.502	21
1.287	0.001259	0.147	0.726	0.853	0.273	0.370	0.647	0.508	19
0.783	0.001531	0.510	0.649	0.490	0.350	0.505	0.589	0.547	17
0.582	0.002922	0.655	0.256	0.345	0.743	0.592	0.402	0.497	23
0.173	0.001638	0.950	0.619	0.050	0.380	0.910	0.568	0.739	6
0.641	0.00053	0.613	0.932	0.387	0.067	0.564	0.882	0.723	7
0.905	0.003371	0.422	0.130	0.578	0.869	0.464	0.365	0.415	28
1.232	0.000392	0.187	0.971	0.813	0.028	0.381	0.947	0.664	12
0.104	0.003478	1.000	0.099	0.000	0.900	1.000	0.357	0.679	11
0.266	0.00165	0.883	0.616	0.117	0.383	0.811	0.566	0.688	10
1.259	0.001455	0.167	0.671	0.833	0.328	0.375	0.604	0.489	25
1.048	0.001543	0.319	0.646	0.681	0.353	0.424	0.586	0.505	20
1.165	0.001719	0.235	0.596	0.765	0.403	0.395	0.554	0.475	26
0.389	0.000557	0.795	0.925	0.205	0.074	0.709	0.870	0.790	3
0.119	0.001914	0.989	0.541	0.011	0.458	0.979	0.522	0.750	5
0.683	0.000294	0.583	0.999	0.417	0.000	0.545	1.000	0.772	4
1.388	0.000369	0.074	0.978	0.926	0.021	0.351	0.959	0.655	13
1.491	0.00049	0.000	0.944	1.000	0.055	0.333	0.900	0.617	15
1.342	0.002377	0.107	0.410	0.893	0.589	0.359	0.459	0.409	29
0.284	**0.000402**	**0.870**	**0.968**	**0.130**	**0.031**	**0.794**	**0.942**	**0.868**	**1**
0.873	0.001896	0.446	0.546	0.554	0.453	0.474	0.525	0.500	22
0.67	0.002579	0.592	0.353	0.408	0.646	0.551	0.436	0.494	24

Optimized Parameters -GRA

The **Table 9** shows the optimized value attained for multi-objective function based on GRA. From the computation it is observed that run 27 is the optimized parameter as shown below:

Table 9. Optimized Parameters - GRA

A	**B**	**C**	**D**	**R_a**	**M_{rr}**
3	15	2	40	0.284	0.000402

IX. CONFIRMATORY RUNS

The validation of the optimized values obtained was confirmed through the execution of confirmatory runs. Trial runs were conducted for both single-objective and multi-objective optimized parameter settings, and the results are presented in **Table 10**.

Table 10. Confirmatory Runs

Tool	**Type**	**Predicted**		**Achieved**	
		Dry run R_a	**Dry run M_{rr}**	**Dry run R_a**	**Dry run M_{rr}**
BBD	Single response **(R_a)**	0.027	-	0.029	-
	Single Response **(M_{rr})**	-	0.004	-	0.039
	Single Response **(P_c)**	-	-	-	**-**
GRA	Multi-response	0.284	0.00402	0.286	0.004

	% Deviation			
Single Response (R_a)	**0.7**			
Single Response (M_{rr})	**8.75**			
Multi-response (GRA)	**R_a**	**0.7**	**M_{rr}**	**0.49**

Table 10 showcases the percentage deviation recorded, confirming the effectiveness of the predicted optimized values. Both the single-response and multi-response optimized levels were found to be satisfactory and acceptable, as their deviation is within 10%.

X. CONCLUSION

The study is performed as single response and multi-response optimization. For single response BBD design is followed and for multi-response GRA is applied. The following are the inferences noted in the entire study and found to be acceptable in accord to the results attained in confirmatory runs:

i) For achieving minimum roughness, Bplays the dominant role followed by C and D
ii) The least contributing factor governing roughness in this case, is found to be A
iii) From table 10, minimum R_a achieved is 0.029 microns under single response method
iv) For maximum M_{rr}, C and D played the prominent role
v) In single response, maximum M_{rr} achievable is 0.039
vi) In case of multi-response optimization, GRA results prediction stands good with minimum R_a of 0.286 microns, maximum M_{rr} of 0.004 mm^3/min

References

[1]. Gohil, V. and Puri, Y.M., 2018. Statistical analysis of material removal rate and surface roughness in electrical discharge turning of titanium alloy (Ti-6Al-4V). Proceedings of the Institution of Mechanical Engineers, Part B: Journal of Engineering Manufacture, 232(9), pp.1603-1614.

[2]. Mohanty, C.P., Satpathy, M.P., Mahapatra, S.S. and Singh, M.R., 2018. Optimization of cryo-treated EDM variables using TOPSIS-based TLBO algorithm. Sādhanā, 43, pp.1-18.

[3]. Mohanty, C.P., Mahapatra, S.S. and Singh, M.R., 2017. An intelligent approach to optimize the EDM process parameters using utility concept and QPSO algorithm. Engineering Science and Technology, an international journal, 20(2), pp.552-562.

[4]. Bhaumik, M. and Maity, K., 2018. Effect of different tool materials during EDM performance of titanium grade 6 alloy. Engineering Science and Technology, an International Journal, 21(3), pp.507-516.

[5]. Mishra, D.K., Datta, S. and Masanta, M., 2018. Effects of tool electrode on EDM performance of Ti-6Al-4V. Silicon, 10, pp.2263-2277.

[6]. Raza, M.H., Wasim, A., Ali, M.A., Hussain, S. and Jahanzaib, M., 2018. Investigating the effects of different electrodes on Al6061-SiC-7.5 wt% during electric discharge machining. The International Journal of Advanced Manufacturing Technology, 99, pp.3017-3034.

[7]. Kumari, S., Datta, S., Masanta, M., Nandi, G. and Pal, P.K., 2018. Electro-discharge machining of Inconel 825 super alloy: effects of tool material and dielectric flushing. Silicon, 10, pp.2079-2099.

[8]. Sadagopan, P. and Mouliprasanth, B., 2017. Investigation on the influence of different types of dielectrics in electrical discharge machining. The International Journal of Advanced Manufacturing Technology, 92(1-4), pp.277-291.

[9]. Li, C., Xu, X., Li, Y., Tong, H., Ding, S., Kong, Q., Zhao, L. and Ding, J., 2019. Effects of dielectric fluids on surface integrity for the recast layer in high speed EDM drilling of nickel alloy. Journal of Alloys and Compounds, 783, pp.95-102.

[10]. Barenji, R.V., Pourasl, H.H. and Khojastehnezhad, V.M., 2016. Electrical discharge machining of the AISI D6 tool steel: Prediction and modeling of the material removal rate and tool wear ratio. Precision Engineering, 45, pp.435-444.

[11]. Soundhar, A., Zubar, H.A., Sultan, M.T.B.H.H. and Kandasamy, J., 2019. Dataset on optimization of EDM machining parameters by using central composite design. Data in brief, 23, p.103671.

[12]. Gaikwad, V. and Jatti, V.S., 2018. Optimization of material removal rate during electrical discharge machining of cryo-treated NiTi alloys using Taguchi's method. Journal of King Saud University-Engineering Sciences, 30(3), pp.266-272.

[13]. Khanna, R., Kumar, A., Garg, M.P., Singh, A. and Sharma, N., 2015. Multiple performance characteristics optimization for Al 7075 on electric discharge drilling by Taguchi grey relational theory. Journal of Industrial Engineering International, 11, pp.459-472.

[14]. Selvarajan, L., Manohar, M., Udhaya Kumar, A. and Dhinakaran, P., 2017. Modelling and experimental investigation of process parameters in EDM of Si 3 N 4-TiN composites using GRA-RSM. Journal of Mechanical Science and Technology, 31, pp.111-122.

[15]. Hegab, H.A., Gadallah, M.H. and Esawi, A.K., 2015. Modeling and optimization of Electrical Discharge Machining (EDM) using statistical design. Manufacturing Review, 2, p.21.

[16]. Świercz, R., Oniszczuk-Świercz, D. and Chmielewski, T., 2019. Multi-response optimization of electrical discharge machining using the desirability function. Micromachines, 10(1), p.72.

[17]. Ray, A., 2016. Optimization of process parameters of green electrical discharge machining using principal component analysis (PCA). The International Journal of Advanced Manufacturing Technology, 87(5-8), pp.1299-1311.

[18]. Sahu, S.N. and Nayak, N.C., 2018. Multi-criteria decision making with PCA in EDM of A2 tool steel. Materials Today: Proceedings, 5(9), pp.18641-18648.

[19]. Dewangan, S., Gangopadhyay, S. and Biswas, C.K., 2015. Study of surface integrity and dimensional accuracy in EDM using Fuzzy TOPSIS and sensitivity analysis. Measurement, 63, pp.364-376.

[20]. Tripathy, S. and Tripathy, D.K., 2016. Multi-attribute optimization of machining process parameters in powder mixed electro-discharge machining using TOPSIS and grey relational analysis. Engineering Science and Technology, an International Journal, 19(1), pp.62-70.

[21]. Sharma, N., Singh, G., Gupta, M., Hegab, H. and Mia, M., 2019. Investigations of surface integrity, bio-activity and performance characteristics during wire-electrical discharge machining of Ti-6Al-7Nb biomedical alloy. Materials Research Express, 6(9), p.096568.

[22]. Dey, A., Debnath, M. and Pandey, K.M., 2017. Analysis of effect of machining parameters during electrical discharge machining using Taguchi-based multi-objective PSO. International Journal of Computational Intelligence and Applications, 16(02), p.1750010.

[23]. Azadi Moghaddam, M. and Kolahan, F., 2020. Modeling and optimization of the electrical discharge machining process based on a combined artificial neural network and particle swarm optimization algorithm. Scientia Iranica, 27(3), pp.1206-1217.

[24]. Torres, A., Puertas, I. and Luis, C.J., 2016. EDM machinability and surface roughness analysis of INCONEL 600 using graphite electrodes. The International Journal of Advanced Manufacturing Technology, 84, pp.2671-2688.
[25]. Datta, S., Biswal, B.B. and Mahapatra, S.S., 2019. Machinability analysis of Inconel 601, 625, 718 and 825 during electro-discharge machining: on evaluation of optimal parameters setting. Measurement, 137, pp.382-400.